HHS Public Access

Author manuscript

J Environ Sci Health B. Author manuscript; available in PMC 2019 August 05.

Published in final edited form as:

J Environ Sci Health B. 2019 ; 54(6): 514–524. doi:10.1080/03601234.2019.1604039.

Development of enterosorbents that can be added to food and water to reduce toxin exposures during disasters

Meichen Wang, **Sara E. Hearon**, **Timothy D. Phillips**

Veterinary Integrative Biosciences Department, College of Veterinary Medicine and Biomedical Sciences, Texas A&M University, College Station, Texas, USA

Abstract

Humans and animals can be exposed to mixtures of chemicals from food and water, especially during disasters such as extended droughts, hurricanes and floods. Drought stress facilitates the occurrence of mycotoxins such as aflatoxins B_1 (AfB_1) and zearalenone (ZEN), while hurricanes and floods can mobilize toxic soil and sediments containing important pesticides (such as glyphosate). To address this problem in food, feed and water, we developed broad-acting, clay-based enterosorbents that can reduce toxin exposures when included in the diet. In this study, we processed sodium and calcium montmorillonite clays with high concentrations of sulfuric acid to increase surface areas and porosities, and conducted equilibrium isothermal analyses and dosimetry studies to derive binding parameters and gain insight into: (1) surface capacities and affinities, (2) potential mechanisms of sorption, (3) thermodynamics (enthalpy) of toxin/surface interactions and (4) estimated dose of sorbent required to maintain toxin threshold limits. We have also used a toxin-sensitive living organism (*Hydra vulgaris*) to predict the safety and efficacy of newly developed sorbents. Our results indicated that acid processed montmorillonites were effective sorbents for AfB_1, ZEN and glyphosate, with high capacity and tight binding, and effectively protected hydra against individual toxins, as well as mixtures of mycotoxins.

Keywords

Sorbents; adsorption; APMs; aflatoxin; zearalenone; glyphosate; isotherm; isothermal analysis; hydra bioassay

Introduction

Humans and animals can be unintentionally exposed to mixtures of hazardous chemicals through contaminated food and water supplies during droughts and floods. Food is susceptible to contaminants during droughts and extended periods of heat, when fungi can reach their optimal growth conditions for the production of mycotoxins.[1] Global warming promotes drought-stressed crops and mold growth, thus enhancing the threat of high-level mycotoxin contamination of the food supply. Moreover, the consumption of these toxins in

CONTACT Timothy D. Phillips tphillips@cvm.tamu.edu Veterinary Integrative Biosciences Department, College of Veterinary Medicine and Biomedical Sciences, Texas A&M University, College Station, TX 77843-4458, USA.

Color versions of one or more of the figures in the article can be found online at www.tandfonline.com/lesb.

the diet can increase the incidence of disease and lethality (especially in the young) during outbreaks. Among the most important toxic mycotoxins occurring in food, aflatoxin B_1 (AfB_1) and zearalenone (ZEN) are widely distributed in cereal crops, including corn, barley, oats, peanuts and wheat. During extended periods of droughts, humans and animals consuming mycotoxin-contaminated diets are vulnerable to the adverse effects of these toxins, including growth stunting, immunosuppression, hepatotoxicity, reproductive defects, cancer and death.[2–4]

During disasters (such as hurricanes and floods), water and food can be contaminated with common pesticides such as glyphosate (among other contaminants). Glyphosate is one of the most frequently used herbicides to control weeds. It has been detected in air during spraying, as well as in water and food. Glyphosate has been detected in the blood and urine of agricultural workers, indicating absorption.[5] Glyphosate is a contemporary issue due to its widespread use, distribution and potential carcinogenicity, including the risk of non-Hodgkin lymphoma and other hematopoietic cancers.[6–8] Glyphosate's mode of action involves inhibition of enzymes associated with the synthesis of three amino acids: tyrosine, tryptophan and phenylalanine. Therefore, it is effective on actively growing plants, but not as a pre-emergence herbicide. The molecular space-filling models for each of these chemicals are shown in Figure 1. They were energy-minimized using a computational quantum mechanical AM1 method (Hyperchem 8.0).[9]

Previously, our laboratory has conducted extensive intervention trials showing that montmorillonite clays, when included in the diet, are able to decrease aflatoxin exposure, toxicity and lethality in young animals and significantly reduce biomarkers of aflatoxin exposure from blood and urine in humans.[10–13] The mechanism for this protection involves tight adsorption of toxins into pores and onto active surfaces of sorbents within the gastrointestinal tract, resulting in decreased toxin bioavailability and toxicity.[14] Additionally, these studies have shown that the inclusion of montmorillonite clay had neither impact on the palatability (texture, taste and odor) nor acceptability of the diet.[15] As indicated above, montmorillonite clays are very effective binders for aflatoxin, but have very limited ability to adsorb other toxins. Currently, no sorbents have been shown to decrease the bioavailability of ZEN from contaminated diets, or glyphosate from contaminated water and food in humans and animals. Previously, a variety of sorbents have been tested for ZEN and glyphosate binding *in vitro*; however, our work is the first to investigate the efficacy of a potential enterosorbent for these toxins using a living organism. To address this problem, our research has focused on the development of novel, clay-based sorbents containing active surfaces that are broad-acting for a variety of important toxins, such as AfB_1, ZEN and glyphosate. Based on previous literature, the treatment of clays, such as montmorillonites, with acid results in the exchange of interlayer cations with protons from the acid, following the partial dissociation of octahedral and tetrahedral sheets in the clay structure. The final reaction product of acid processed montmorillonite clays (APMs) is thought to be a mixture of delaminated parent clay layers containing chains of amorphous silica on the edges, amorphous silica and crosslinked silica (Fig. 2).[16–18] The pH of the final APM product is approximately 3, which is similar to acidic foods such as meat, cheese and chocolate. In fact, the inclusion of acidic food additives can serve as a common taste enhancer and increase palatability and consumption.[19] Also, acids, such as sulfuric acid, are permitted as food and

feed additives to adjust pH.[20,21] Thus, the inclusion of APMs at a low concentration in the diet of humans and animals for short-term treatments should be safe. A variety of acid processed clays have already been developed and used extensively for bleaching purposes,[22] removal of plant pigments from oils[23] and sequestering various organic and inorganic contaminants from water during decontamination and purification procedures.[24–26] However, there are no reports suggesting that these types of materials (APMs) might be included in the diets of animals and humans for short-term treatment to decrease exposure to toxins from contaminated water and food.

To determine the binding efficacy of APMs, we conducted equilibrium isothermal analyses and dosimetry studies to derive binding parameters and gain insight into: (1) surface capacity and affinity, (2) potential mechanisms of sorption, (3) thermodynamics of toxin/surface interactions and (4) estimated dose of sorbent required to maintain threshold limits. We have also used a toxin-sensitive living organism (*Hydra vulgaris*) to predict the *in vivo* safety and efficacy of APMs and their ability to mitigate the toxicity of commonly occurring mycotoxins and pesticides.

Materials and methods

Reagents

High pressure liquid chromatography (HPLC) grade acetonitrile, reagents and pH buffers (4.0, 7.0 and 10.0) were purchased from VWR (Atlanta, GA). AfB_1, ZEN and glyphosate were purchased from Sigma Aldrich (Saint Louis, MO). Sulfuric acid (H_2SO_4, 95–98%) and formic acid (HCOOH, 88%) were purchased from Aldrich Chemical Co. (Milwaukee, WI). In this study, a calcium montmorillonite (CM) was obtained from Engelhard Corp. (Cleveland, OH) with an average total surface area as high as 850 $m^2\ g^{-1}$, an external surface area of approximately 70 $m^2\ g^{-1}$ and cation exchange capacity equal to 97 cmol kg^{-1}.[1] Sodium montmorillonite (SM) was a gift from the Source Clay Minerals Repository at the University of Missouri-Columbia with cation exchange capacity equal to 75 cmol kg^{-1}. The generic formula for these clays is: $(Na,Ca)_{0.3}(Al,Mg)_2Si_4O_{10}(OH)_2{\cdot}nH_2O$. Samples of both clays contain some quartz, mica, calcite, orthoclase feldspars and sanidine as impurities, and mesopores of approximately 5 nm in diameter.[27] Ultrapure deionized water (18.2 MX) was generated in the lab using an Elga™ automated filtration system (Woodridge, IL) and was used in all experiments.

Synthesis of sorbents

CM and SM were treated with sulfuric acid to produce broad-acting sorbents with high surface areas and porosities. In glass beakers, 5 g (6%) of CM and SM clay mineral suspensions were individually treated with 12 N or 18 N sulfuric acid. The solutions were vigorously stirred and kept in an oven at 60 °C overnight. The slurry was cooled, centrifuged at 2000*g* for 20 min and washed thoroughly with distilled water. This centrifugation–washing process was repeated multiple times until the pH for each treatment group was constant. All samples were dried in the oven at 110 °C overnight before grinding and sieving through a 125-μm screen. These grinding and sieving steps were necessary to obtain clay particles of uniform size.[25,28]

To investigate the binding of toxins to sorbent surfaces and to determine the importance of intact clay interlayers, experiments with heat-collapsed sorbents were also conducted. Collapsed sorbents were prepared by heating APMs at 200°C for 30 min followed by 800°C for 1 h to collapse the interlayer.[29]

In vitro isothermal adsorption

The toxin stock solution was prepared by dissolving pure crystals into acetonitrile. Aliquots of the solution were injected into a sample of distilled water (pH 6.5) for each toxin to yield 8 ppm (8 μg mL^{-1}) AfB_1, 4 ppm ZEN and 10 ppm glyphosate solutions. The concentrations were established based on the octanol–water partitioning coefficients (K_{ow}) so that precipitation during the testing was not a factor, and the optimal toxin/sorbent ratio was designed to fit the Langmuir model. Then 0.002% (wt/vol) of sorbents was exposed to an increasing concentration gradient of toxin in solution. In all assays, besides test samples, there were three controls consisting of distilled water, toxin solution without sorbent and sorbent solution without toxin. The control and test groups in disposable glass tubes were capped and agitated at 1000 rpm for 2 h at either 24 °C (T_1) or 37 °C (T_2) using an electric shaker. All samples were then centrifuged at 2000*g* for 20 min to separate the sorbent/toxin complex from solution. The UV–visible scanning spectrophotometer was used to scan and read the adsorption peak at 362 nm for AfB_1 and 236 nm for ZEN.[1,3]

Glyphosate was analyzed using a Waters Acquity® Ultra Performance Liquid Chromatography (UPLC)-Mass Spectrometry (MS)/MS equipped with a BEH C18 column (50 × 2.1 mm). Separation was obtained with a mobile phase of water with 0.1% formic acid (eluate A) and acetonitrile with 0.1% formic acid (eluate B) (5%–100% of eluate B in 10 min) at 0.3 mL min^{-1} with a 40 μL injection volume and a negative electrospray ionization mode at 4.5 kV spray voltage. Nitrogen gas was used as the collision gas and curtain gas, and argon gas was used as the nebulizer gas and heater gas. The source temperature was kept at 225 °C. The mass spectrometer was operated under multiple reaction monitoring (MRM) mode and the monitored precursor and product ions were 168 and 63/81. The unit mass resolution was used for the ion mass analyzer. Empower analyst software was used to control the LC/MS/MS system and acquire the data.[30] To validate this detection method for glyphosate, a standard solution of glyphosate was prepared in distilled water at concentrations between 20 ppm and 0.5 ppm to measure the standard curves. The standard curve for glyphosate is linear ($r^2 > 0.99$), and described by Eq. (1).

$$y = 32{,}185x + 41{,}034 \quad (1)$$

where: x is the glyphosate concentration (ppm) and y is the signal intensity from LC/MS/MS.

Data calculations and curve fitting

Glyphosate concentrations in solution were detected by LC/MS/MS and calculated from peak area. A UV–visible scanning spectrophotometer was used to calculate the concentration of AfB_1 and ZEN left in solution (c) using Beer's law ((Eq. (2)).

$$\text{Beer's law Absorbance} = e \cdot L \cdot c \quad (2)$$

where: e is the molar extinction coefficient (e for AfB_1 = 21,865 cm^{-1} mol^{-1}, e for ZEN = 24,833 cm^{-1} mol^{-1}), L is the path length of the cell holder = 1 cm.

The amount adsorbed for each data point was calculated from the concentration difference between test and control groups. More specifically, the *y*-axis is the amount of toxin bound by sorbents (in mol kg^{-1}). It is calculated by the difference in moles of free toxin in the test solution versus control groups and is then divided by the mass of the sorbents included. These data were then plotted using Table-Curve 2D and a computer program that was developed with Microsoft Excel to derive values for the variable parameters. The best fit for the data was a Langmuir model, which was used to plot equilibrium isotherms from triplicate analysis. The isotherm equation was entered as user-defined functions:

$$\text{Langmuir model } q = Q_{\max}\left(\frac{K_d C_w}{1 + K_d C_w}\right) \quad (3)$$

where: q = toxin adsorbed (mol kg^{-1}), Q_{max} = maximum capacity (mol kg^{-1}), K_d = distribution constant, C_w = equilibrium concentration of toxin.

The plot will normally display a break in the curve. The value on the *x*-axis where the curve breaks is an estimate of K_d^{-1} The value on the *y*-axis where the curve breaks is an estimate of Q_{max}. The definition of K_d is derived from the Langmuir equation giving:

$$K_d = \frac{q}{(Q_{\max} - q)C_w} \quad (4)$$

The enthalpy (ΔH) was calculated by comparing the difference of K_d values at 24 °C (T_1) and 37 °C (T_2) by the following equation:

$$\text{Van}' \text{ t Hoff equation } \Delta H_{ads} = \frac{-R \ln\left(\frac{K_{d2}}{K_{d1}}\right)}{\left(\frac{1}{T_2}\right) - \left(\frac{1}{T_1}\right)} \quad (5)$$

where: R (ideal gas constant) = 8.314 J mol^{-1} K^{-1}, T = absolute temperature (K).

Dose of sorbents required to maintain threshold limits of toxins

In the dosimetry study, ZEN and glyphosate were diluted with distilled water from a stock solution to derive 2 ppm ZEN and 20 ppm glyphosate solutions that were set at twice their threshold limits (ZEN in food = 1 ppm; glyphosate in water and food = 10 ppm).[31,32] An

increasing gradient of sorbent inclusion was added to 5.0 mL of ZEN solution at 0.005, 0.02, 0.05, 0.2, 1.0 mg mL^{-1}, and glyphosate at 0.02, 0.1, 0.5, 1.0, 2.0 mg mL^{-1}. Control groups included distilled water and toxin solution without sorbent. Both control and test groups in disposable glass tubes were capped and agitated at 1000 rpm for 2 h. All samples were then centrifuged at 2000g for 20 min. Aliquots of ZEN were read on a UV–visible scanning spectrophotometer at 236 nm and calculated by Beer's law ((Eq. (2)) for the remaining (unbound) ZEN concentration. Aliquots of glyphosate were measured by LC/MS/MS and calculated by the signal peak area for the remaining glyphosate concentration. The toxin sorption percentage was calculated by the difference between control and test groups. Predicted algorithms were derived to extrapolate the sorbent inclusion levels required to meet the threshold limits for ZEN in food and glyphosate in water and food.

Hydra bioassay

H. vulgaris were obtained from Environment Canada (Montreal) and maintained at 18 °C. The hydra classification method[33] was used with modification[34] to rate morphology of the adult hydra as an indicator of toxicity. Mature and non-budding hydra in similar sizes were chosen for testing in order to minimize the differences between samples. Toxin treatment groups included 20 ppm AfB_1, 4 ppm ZEN and 30 ppm glyphosate in the hydra media based on the minimum effective dose of each toxin resulting in 100% mortality in 92 h. Toxin mixture treatment groups included 1 ppm AfB_1 and 6 ppm ZEN based on the ratio of average concentrations of AfB_1 and ZEN reported worldwide in animal feedstuffs.[4] The combination of the two mycotoxins (ZEN and AfB_1) was tested in the hydra bioassay, since these mycotoxins tend to commonly occur in food and feed together, especially during outbreaks of drought. All test solution tubes were capped and prepared by shaking at 1000 rpm for 2 h and centrifugation at 2000*g* for 20 min prior to exposure to hydra in pyrex dishes to toxin. For each sample, three hydra were included into 4 mL of test media and kept at 18 °C. Hydra solutions were not changed throughout the 92-h testing period. The assay included monitoring times at shorter intervals during the first two days (0, 4, 20 and 28 h) and 24 h intervals for the last three days (44, 68 and 92 h).[35] The hydra morphological response was scored and recorded after exposure to toxin, with and without sorbent treatment. The toxicity rating was determined by calculating the average score for morphological changes for a certain group at a specific time point.

Statistical analysis

A two-way t-test was used to calculate statistical significance. Each experiment was triplicated to derive an average and standard deviation. In the *t*-test, Q_{max} from heat collapse analyses and toxicity scores from the hydra bioassay were included to calculate *t*-values. The *t*-value and degrees of freedom were compared in a *P*-value table to determine the statistical significance. Results were considered significant at $P \leq 0.05$.

Results and discussion

Figure 1 illustrates the chemical structures and molecular models of AfB_1 (Fig. 1A), ZEN (Fig. 1B) and glyphosate (Fig. 1C). Figure 2 shows the energy minimized molecular models

of parent montmorillonite clay versus moderately and highly processed APMs, illustrating the process and the products of acid treatment.

Equilibrium isotherms were generated by Table-Curve 2D and a computer program developed in our laboratory using Microsoft Excel to derive affinities (K_d), capacities (Q_{max}) and the enthalpies (ΔH) of sorption for toxin–surface interactions. Figure 3A shows the isothermal plot for AfB_1 on the surfaces of acid processed CM (APCM). Figure 3B shows the isothermal plot for AfB_1 on the surfaces of acid processed SM (APSM). The r^2 values (>0.8) for the Langmuir model and saturable plots indicate that AfB_1 binds tightly onto clay surfaces and does not dissociate easily. The derived Q_{max} values indicated that APMs were able to bind AfB_1 like the parent clays. Based on previous studies, sorbents such as SM had high expansibility in water with enhanced access to active surfaces resulting in a higher K_d for AfB_1 versus APSM. To calculate the sorption enthalpies of APM clays for AfB_1, thermodynamic isotherms were run at two different temperatures, i.e. 24 °C (T_1) and 37 °C (T_2). Calculated enthalpies (ΔH) for APCM-12N, APCM-18N, APSM-12N and APSM-18N were equal to −100 kJ mol^{-1}, −67 kJ mol^{-1}, −135 kJ mol^{-1} and −131 kJ mol^{-1}, respectively (Fig. 3C,D). These findings indicate that AfB_1 was chemisorbed tightly to the clay surfaces and it is consistent with the Langmuir model for the interaction. The minus symbol suggests that the reaction is spontaneous in the forward direction to form toxin/adsorbent product. Since the absolute values were more than the minimum level for chemisorption (i.e. 20 kJ mol^{-1}), data suggest that the adsorption reaction is a chemisorption involving tight binding, not physisorption. The safety and efficacy of sorbents were further confirmed using the hydra bioassay (Fig. 3E). Following the inclusion of CM and APCM at a 0.005% inclusion level, adult hydra were completely protected from aflatoxin toxicity with no morphological and physiological changes from the hydra media control group.

Figure 4 shows the isotherms for ZEN adsorption on the surfaces of APCM and APSM, respectively. Freundlich isotherms in Figure 4A,B suggests that ZEN adsorption onto the surfaces of parent CM and SM clays shows a linear trend, which indicates partitioning activity, instead of tight binding at saturable sites. APMs were able to improve ZEN binding with saturable curves that fit the Langmuir model ($r^2 > 0.8$), which indicate tight binding onto active clay surfaces. The high binding capacity ($Q_{max} > 0.2$) suggests the ability of APMs to serve as effective ZEN enterosorbents; this effect is probably due to higher surface areas (and more porosity) than that of parent clays. The hydra data in Figure 4C shows the significantly enhanced binding of ZEN onto APM surfaces at an inclusion rate of 0.01% that resulted in complete protection against ZEN toxicity. The parent clay (CM) showed no protection against ZEN toxicity at the same inclusion rate.

The APMs were collapsed with heat to determine the importance of the interlayer space for AfB_1 and ZEN sorption, singly and in combination. After heating clays at 800 C, the interlayers were dehydroxylated and collapsed.[1] Figure 5A shows that binding capacities for AfB_1 on collapsed APMs were significantly reduced, with 20% and 14% of aflatoxin remaining on collapsed (Co) APCM-12N and APCM-18N, respectively. This dramatic decrease of AfB_1 suggests that more than half of the AfB_1 binds within the intact interlayers available in the processed sorbents as predicted from thermodynamic calculations and computational modeling. Based on the partial positive charge on carbons C11 and C1 of the

AfB_1 dicarbonyl system and the strength of adsorption of planar analogs and derivatives of AfB_1, an electron donor–acceptor mechanism was postulated for the AfB_1 sorption mechanism onto the negatively charged montmorillonite interlayer. On the other hand, Figure 5B shows that the percentages of the ZEN remaining on collapsed clays were 50% and 63% (i.e. CoAPCM-12N and CoAPCM-18N, respectively). Unlike AfB_1, less than half of the ZEN binds within the intact interlayers in the processed sorbents indicating the potential for significant binding to sites other than the interlayer. This difference in binding sites for ZEN is possibly due to its hydrophobic nature with a log P (octanol–water) equal to 3.6 and neutral charge. Despite this difference in binding sites, both the adsorption isotherms of AfB_1 and ZEN indicate tight binding and the binding site is saturable with toxins. To investigate the ability of APMs to protect against combinations of AfB_1 and ZEN, adult hydra were exposed to a common toxin mixture of 1 ppm AfB_1 and 6 ppm ZEN, based on an worldwide average AfB_1 and ZEN concentrations reported in animal feedstuffs (Fig. 5C). The inclusion of APMs at 0.1% wt/wt significantly prevented the mortality of hydra with 90% and 100% protection from APCM-12N and APCM-18N, respectively. The slight protection by parent CM is in alignment with the *in vitro* isothermal results indicating that the parent CM can bind AfB_1, but not ZEN. APMs were shown to significantly protect the hydra from AfB_1 and ZEN confirming simultaneous sorption of both toxins, with limited interference. Importantly, this finding suggests that APMs may be able to decrease exposures to foodborne toxins in humans and animals when included in the diet.

The widespread occurrence of ZEN in food and feed is commonly associated with severe drought and adverse impacts to health. There are no clay-based sorbents, or other treatments, to prevent disease and death from this toxin. Thus, to develop an optimal toxin enterosorbent for ZEN, it is important to gain insight into the binding efficacy and the thermodynamics of the interaction of this toxin on active surfaces of APMs. To calculate the binding enthalpy of APMs for ZEN, isotherms for ZEN were run at 24 °C and 37 °C. Calculated enthalpies (ΔH) for APCM-12N, APCM-18N, APSM-12N and APSM-18N were equal to −90 kJ mol^{-1}, −75 kJ mol^{-1}, −74 kJ mol^{-1} and −78 kJ mol^{-1}, respectively (Fig. 6A,B). Based on the minus symbol and the high absolute values (>20 kJ mol^{-1}), data suggest that the adsorption reaction is a chemisorption involving tight binding, not physisorption

Additionally, we conducted a study to determine the dose of APMs that could be used to treat humans and animals during droughts and outbreaks of ZEN toxicosis. The regulatory threshold for ZEN in food in the U.S. is equal to 1.0 ppm. Based on our dosimetry results (Fig. 6C), the predicted inclusion rates were equal to 1.0 g kg^{-1} and 0.73 g kg^{-1} (wt/wt of diet) for APCM-12N and APCM-18N, respectively. These results suggest that a low dose of APMs would be required for treatment and could serve as an effective sorbent to decrease ZEN exposure when administered before each meal. This low inclusion rate was derived from the isothermal results and confirmed in the hydra bioassay. This information will help to facilitate a determination of dosage requirements for enterosorbent treatment in animals and humans for ZEN during outbreaks.

Glyphosate is one of the most widely used herbicides and has been detected in water and food. During hurricanes and floods, glyphosate (and other environmental chemicals) may be mobilized and redistributed from soil and sediment at the site of these disasters into

vulnerable communities. Therefore, strategies to reduce unintentional exposures of humans and animals to glyphosate (and other) potential carcinogens[7] during disasters are warranted.

Our isothermal results in Figure 7A,B showed significantly increased glyphosate binding capacities for APMs compared to the parent clays. This high binding efficacy is further confirmed by the hydra bioassay (Fig. 7C,D), where APMs at the inclusion rate at 0.1% were able to completely protect hydra against glyphosate toxicity, whereas the parent SM was shown to have limited protection. The results of a thermodynamic study of glyphosate adsorption in Figure 8A showed binding enthalpies of SM, APSM-12N and APSM-18N equal to −36 kJ mol^{-1}, −37 kJ mol^{-1} and −22 kJ mol^{-1}, respectively. This finding indicates that the adsorption of glyphosate is spontaneous in the forward direction and involves chemisorption, or tight binding onto active clay surfaces. To determine the dose to maintain a threshold limit for glyphosate and facilitate the decision of dosage forms for treatment, a dosimetry study was conducted (Fig. 8B). In this study, a NOEL (no observed effect level) in food and water was used as the threshold limit for glyphosate due to its probable carcinogenicity. Based on our results, the required doses for APCM-12N and APCM-18N were 2 g kg^{-1} and 1.38 g kg^{-1}, suggesting increased binding efficacy compared to the predicted dose for CM (i.e. 3.6 g kg^{-1}). Assuming 1 kg of diet is consumed by adults at each meal, then small capsules of APMs, or snacks, vitamins and flavored water containing APMs could be administered before each meal to significantly reduce glyphosate exposure during a disaster. Additionally, APMs may also be added to community garden soils (before and after disasters) to reduce the potential for toxin translocation to plants and dermal exposures from contaminated soil.

APMs had high binding capacity and affinity for AfB_1, ZEN and glyphosate and resulted in complete protection against individual toxins as well as mycotoxin mixtures. With toxin exposure, no morphological and physiological changes were observed in the APM treatment groups. The dose of APMs required to protect hydra and meet the threshold limit for ZEN and glyphosate was lower than the parent clays they were derived from. These findings were predicted by the increased binding capacity for ZEN and glyphosate *in vitro* based on equilibrium isotherms. The mechanisms of APM sorption of toxins likely involve interactions at multiple binding sites on active surfaces of APMs, including partially delaminated clay layers, amorphous silica and crosslinked silica. The heterogeneity of APM surfaces was consistent with a lower correlation ($r^2 > 0.8$) for a homogenous Langmuir plot of the data. The fact that the Langmuir model remained the best fit for the adsorption curves of AfB_1, ZEN and glyphosate, indicated that there was a major binding site with high affinity for each chemical. Earlier work suggested that acid processing of montmorillonite clay significantly increased pore volume and pore diameter resulting in higher surface areas than the parent clay.[36] This study is consistent with these findings in that the total surface area of APMs was increased by 60% from approximately 800 m^2 g^{-1} (for parent clays) to 1300 m^2 g^{-1} (for APM-18N). This increased surface area and porosity was consistent with the broad-acting ability of APMs to bind different toxins. Previous studies have reported that the surfaces of acid processed bentonites (similar to APMs) have both positive and negative charges.[37] These charged surfaces may be partially responsible for the high binding efficacy for neutral chemicals like AfB_1 and ZEN, or zwitterionic chemicals like glyphosate.

Conclusion

The main novelty of this study is the fact that we can utilize APMs that contain surface areas and porosities higher than parent clays as broad-acting toxin enterosorbents for multiple contaminants in food and water, especially at the site of disasters. Based on our previous studies, montmorillonite clay was the most effective aflatoxin sorbent and the only sorbent shown to be safe for human consumption when included in diets, but there are no reports of effective clay-based sorbents to reduce ZEN and glyphosate bioavailability *in vivo*. In this study, novel APMs were shown to bind AfB_1, ZEN and glyphosate with high binding capacity and enthalpy, and completely protected hydra against individual toxins and mycotoxin mixtures. We also estimated the dose of sorbent required to keep exposures below the regulatory threshold level for individual toxins, which will help to determine an optimal dose for short-term treatment. Based on the toxin binding efficacy of APMs for AfB_1, ZEN and glyphosate (*in vitro* and *in vivo*), it is possible that these, and other acid processed clays, may be broad-acting in their ability to decrease exposures to numerous chemical contaminants from food and water such as other pesticides, PAHs, commercial solvents, plasticizers and metals. We anticipate the short-term inclusion of broad-acting APMs in the diet of humans and animals as a protective measure to minimize unintended exposures from contaminated food and water supplies at the site of disasters, including droughts, hurricanes, floods, chemical spills, fires, and acts of terror.

Funding

This work was supported by funding by NIH/NIEHS SRP (Superfund hazardous Substance Research and Training Program), P42 ES0277704 and Texas AgriLife H6215.

References

[1]. Grant PG; Phillips TD Isothermal adsorption of aflatoxin B(1) on HSCAS clay. J. Agric. Food Chem 1998, 46, 599–605. [PubMed: 10554284]

[2]. Avantaggiato G; Greco D; Damascelli A; Solfrizzo M; Visconti A Assessment of multi-mycotoxin adsorption efficacy of grape pomace. J. Agric. Food Chem 2014, 62, 497–507. DOI:10.1021/jf404179h. [PubMed: 24364566]

[3]. Lemke SL; Grant PG; Phillips TD Adsorption of zearalenone by organophilic montmorillonite clay. J. Agric. Food Chem 1998, 46, 3789–3796. DOI: 10.1021/jf9709461.

[4]. Murugesan GR; Ledoux DR; Naehrer K; Berthiller F; Applegate TJ; Grenier B; Phillips TD; Schatzmayr G Prevalence and effects of mycotoxins on poultry health and performance, and recent development in mycotoxin counteracting strategies. Poult. Sci 2015, 94, 1298–1315. DOI: 10.3382/ps/pev075. [PubMed: 25840963]

[5]. Duke SO; Powles SB Glyphosate: A once-in-a-century herbicide. Pest Manag. Sci 2008, 64, 319–325. DOI: 10.1002/ps.1518. [PubMed: 18273882]

[6]. Guyton KZ; El Ghissassi F; Benbrahim-Talaa L; Grosse Y; Loomis D; Straif K Recent progress in mechanistic data evaluation: The IARC monographs perspective. Environ. Mol. Mutagen 2015, 56, 84–84.

[7]. Guyton KZ; Loomis D; Grosse Y; El Ghissassi F; Benbrahim-Tallaa L; Guha N; Scoccianti C; Mattock H; Straif K; International Agency for Research on Cancer Monograph Working Group, IARC, Lyon, France. Carcinogenicity of tetrachlorvinphos, parathion, malathion, diazinon, and glyphosate. Lancet Oncol 2015, 16, 490–491. DOI: 10.1016/S1470-2045(15)70134-8. [PubMed: 25801782]

[8]. International Agency for Research on Cancer. Some Organophosphate Insecticides and Herbicides: Tetrachlorvinphos, Parathion, Malathion, Diazinon and Glyphosate IARC working Group, IARC Monographs on the evaluation of Carcinogenic Risk to Humans: Lyon, 2015; 112.

[9]. Phillips TD; Sarr AB; Grant PG Selective chemisorption and detoxification of aflatoxins by phyllosilicate clay. Nat. Toxins 1995, 3, 204 Discussion 221. [PubMed: 7582618]

[10]. Awuor AO; Yard E; Daniel JH; Martin C; Bii C; Romoser A; Oyugi E; Elmore S; Amwayi S; Vulule J; et al. Evaluation of the efficacy, acceptability and palatability of calcium montmorillonite clay used to reduce aflatoxin B1 dietary exposure in a crossover Study in Kenya. Food Addit. Contam. Part A Chem. Anal. Control Expo. Risk Assess 2017, 34, 93–102. DOI: 10.1080/19440049.2016.1224933. [PubMed: 27603954]

[11]. Maki CR; Haney S; Wang M; Ward SH; Rude BJ; Bailey RH; Harvey RB; Phillips TD Calcium montmorillonite clay for the reduction of aflatoxin residues in milk and dairy products. Dairy Vet. Sci. J 2017, 2, 1–8. DOI: 10.19080/JDVS.2017.02.555587.

[12]. Mitchell NJ; Xue KS; Lin S; Marroquin-Cardona A; Brown KA; Elmore SE; Tang L; Romoser A; Gelderblom WC; Wang JS; et al. Calcium montmorillonite clay reduces AFB1 and FB1 biomarkers in rats exposed to single and co-exposures of aflatoxin and fumonisin. J. Appl. Toxicol 2014, 34, 795–804. DOI: 10.1002/jat.2942. [PubMed: 24193864]

[13]. Pollock BH; Elmore S; Romoser A; Tang L; Kang MS; Xue K; Rodriguez M; Dierschke NA; Hayes HG; Hansen HA; et al. Intervention trial with calcium montmorillonite clay in a south texas population exposed to aflatoxin. Food Addit. Contam. Part A. Chem. Anal. Control Expo. Risk Assess 2016, 33, 1346–1354. DOI: 10.1080/19440049.2016.1198498. [PubMed: 27321368]

[14]. Phillips TD Dietary clay in the chemoprevention of aflatoxin-induced disease. Toxicol. Sci 1999, 52, 118–126. [PubMed: 10630600]

[15]. Awuor AO; Yard E; Daniel JH; Martin C; Bii C; Romoser A; Oyugi E; Elmore S; Amwayi S; Vulule J; et al. Evaluation of the efficacy, acceptability and palatability of calcium montmorillonite clay used to reduce aflatoxin B1 dietary exposure in a crossover study in Kenya. Food Addit. Contam. Part A Chem. Anal. Control Expo. Risk Assess 2017, 34, 93–102. DOI: 10.1080/19440049.2016.1224933. [PubMed: 27603954]

[16]. Komadel P; Schmidt D; Madejová J; CÍcel B Alteration of smectites by treatments with hydrochloric acid and sodium carbonate solutions. App. Clay Sci 1990, 5, 113–122. DOI: 10.1016/0169-1317(90)90017-J.

[17]. Madejova J; Bujdak J; Janek M; Komadel P Comparative FTIR study of structural modifications during acid treatment of dioctahedral smectites and hectorite. Spectrochim. Acta Part A Mol. Biomol. Spectrosc 1998, 54, 1397–1406. DOI: 10.1016/S1386-1425(98)00040-7.

[18]. Tyagi B; Chudasama CD; Jasra RV Determination of structural modification in acid activated montmorillonite clay by FTIR spectroscopy. Spectrochim. Acta Part A Mol. Biomol. Spectrosc 2006, 64, 273–278. DOI: 10.1016/j.saa.2005.07.018.

[19]. Deshpande SA; Yamada R; Mak CM; Hunter B; Obando AS; Hoxha S; Ja WW Acidic food pH increases palatability and consumption and extends drosophila lifespan. J. Nutr 2015, 145, 2789–2796. DOI: 10.3945/jn.115.222380. [PubMed: 26491123]

[20]. Food and Drugs Act. Marketing authorization for food additives that may be used as pH adjusting agents, acid-reacting materials or water correcting agents https://www.canada.ca/en/health-canada/services/food-nutrition/food-safety/food-additives/lists-permitted/10-adjusting-agents.html (accessed Nov. 20, 2018.).

[21]. U.S. Food and Drug Administration. Food additive status list https://www.fda.gov/Food/IngredientsPackagingLabeling/FoodAdditivesIngredients/ucm091048.htm (accessed Nov. 20, 2018.).

[22]. De BK; Patel JD; Patel JB; Patel VK; Patel VR Bleaching of mustard oil with some alternative bleaching agents and acid activated clay. J. Oleo Sci 2009, 58, 57–63. [PubMed: 19145059]

[23]. Yip AC; Lam FL; Hu X A novel heterogeneous acid-activated clay supported copper catalyst for the photobleaching and degradation of textile organic pollutant using photo-fenton-like reaction. Chem. Commun 2005, 25, 3218–3220. DOI: 10.1039/b501531f.

[24]. Ake CL; Mayura K; Huebner H; Bratton GR; Phillips TD Development of porous clay-based composites for the sorption of lead from water. J. Toxicol. Environ. Health A 2001, 63, 459–475. DOI: 10.1080/152873901300343489. [PubMed: 11482800]

[25]. Resmi G; Thampi SG; Chandrakaran S Removal of lead from wastewater by adsorption using acid-activated clay. Environ. Technol 2012, 33, 291–297. DOI: 10.1080/09593330.2011.572917. [PubMed: 22519114]

[26]. Ugochukwu UC; Fialips CI Crude oil polycyclic aromatic hydrocarbons removal via clay-microbe-oil interactions: Effect of acid activated clay minerals. Chemosphere 2017, 178, 65–72. DOI: 10.1016/j.chemosphere.2017.03.035. [PubMed: 28319743]

[27]. Marroquin-Cardona A; Deng Y; Garcia-Mazcorro J; Johnson NM; Mitchell N; Tang L; Robinson A; Taylor J; Wang JS; Phillips TD Characterization and safety of uniform particle size NovaSil clay as a potential aflatoxin enterosorbent. Appl. Clay Sci 2011, 54, 248–257. [PubMed: 22249378]

[28]. Neji SB; Trabelsi M; Frikha MH Esterification of fatty acid over tunisian acid activated clay: Kinetic study. J. Oleo Sci 2011, 60, 293–299. [PubMed: 21606617]

[29]. Wang M; Maki CR; Deng Y; Tian Y; Phillips TD Development of high capacity enterosorbents for aflatoxin B1 and other hazardous chemicals. Chem. Res. Toxicol 2017, 30, 1694–1701. DOI: 10.1021/acs.chemrestox.7b00154. [PubMed: 28768106]

[30]. Loffredo E; Castellana G; Senesi N Decontamination of a municipal landfill leachate from endocrine disruptors using a combined sorption/bioremoval approach. Environ. Sci. Pollut. Res. Int 2014, 21, 2654–2662. DOI: 10.1007/s11356-013-2202-z. [PubMed: 24122163]

[31]. Mazumder PM; Sasmal D Mycotoxins – Limits and regulations. Ancient Sci. Life 2001, 20, 1–19.

[32]. Integrated Risk Information System (IRIS). Glyphosate; CASRN 1071-83-6 U.S. Environmental Protection Agency: Washington, DC, 1987.

[33]. Wilby OK; Tesh JM; Shore PR Application of the hydra regeneration assay: Assessment of the potential teratogenic activity of engine exhaust emissions. Toxicol. In vitro 1990, 4, 612–613. DOI: 10.1016/0887-2333(90)90126-E. [PubMed: 20702240]

[34]. Ottinger SE; Mayura K; Lemke SL; McKenzie KS; Wang N; Kubena LF; Phillips TD Utilization of electrochemically generated ozone in the degradation and detoxification of benzo[a]pyrene. J. Toxicol. Environ. Health Part A 1999, 57, 565–583. DOI: 10.1080/009841099157511. [PubMed: 10515574]

[35]. Brown KA; Mays T; Romoser A; Marroquin-Cardona A; Mitchell NJ; Elmore SE; Phillips TD Modified hydra bioassay to evaluate the toxicity of multiple mycotoxins and predict the detoxification efficacy of a clay-based sorbent. J. Appl. Toxicol 2014, 34, 40–48. DOI: 10.1002/jat.2824. [PubMed: 23047854]

[36]. Rhodes CN; Brown DR Surface properties and porosities of silica and acid-treated montmorillonite catalyst supports: Influence on activities of supported $ZnCl_2$ alkylation catalysts. J. Chem. Soc 1993, 89, 1387–1391.

[37]. Ozcan AS; Ozcan A Adsorption of acid dyes from aqueous solutions onto acid-activated bentonite. J. Colloid Interface Sci 2004, 267, 39–46.

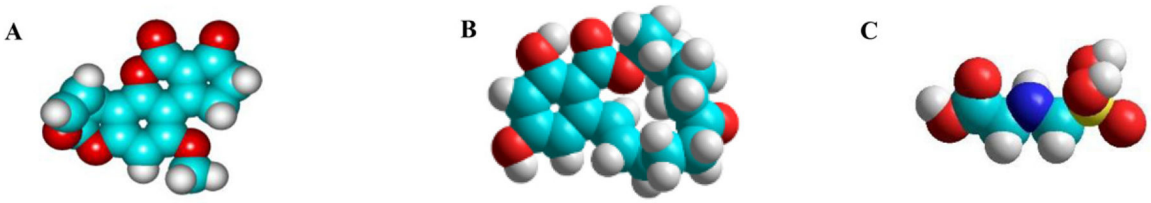

Figure 1.

Chemical structures and molecular models of AfB_1 (A), ZEN (B) and glyphosate (C), illustrating the spatial orientation and size of the functional groups.

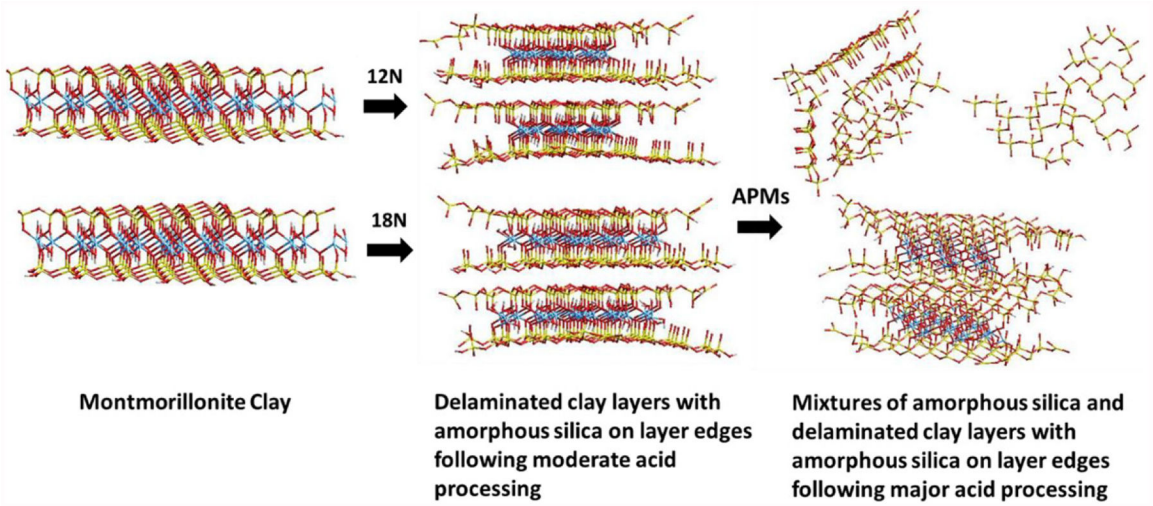

Figure 2.

Energy minimized molecular models of parent montmorillonite clay versus moderately and highly processed APMs, illustrating the process and potential products of acid treatment.

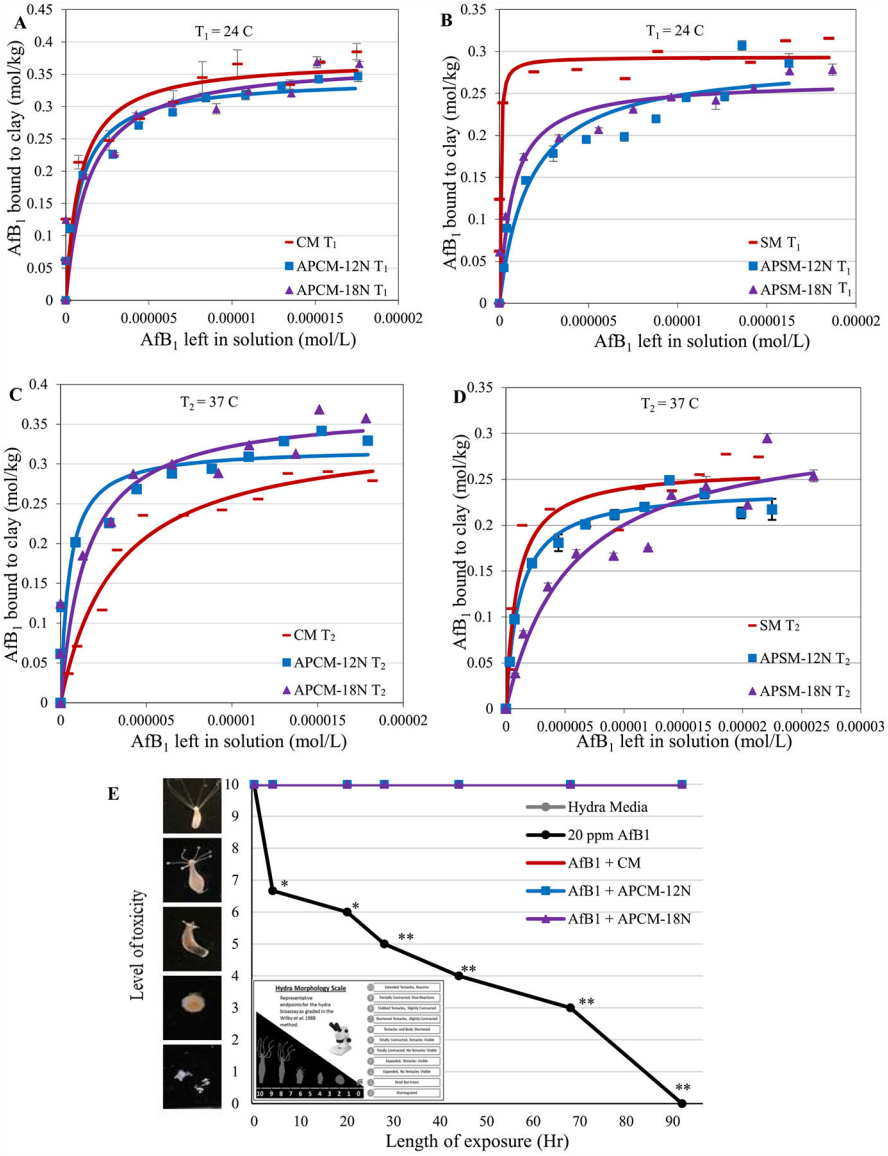

Figure 3.

Langmuir plots of AfB_1 on APCM and APSM versus parent clays showing the observed and predicted Q_{max} values at 24°C (T_1) in A and B and 37 °C (T_2) in C and D. The Q_{max} values indicated tight binding. Hydra toxicity and protection by CM and APCM at 0.005% inclusion level against 20 ppm AfB_1 (E). Hydra media and toxin controls are included for comparison. The score of 10 (indicating no toxicity) contains the hydra media and both APCM treatments ($*P \leq 0.05$, $**P \leq 0.01$). The binding and affinity parameters are as follows: (A) CM T_1: Q_{max} = 0.37; K_d = 1E6; APCM-12N T_1: Q_{max} = 0.34; K_d = 1E6; APCM-18N T_1: Q_{max} = 0.37; K_d = 8E5. (B) SM T_1 Q_{max} = 0.3; K_d = 2E7; APSM-12N T_1. Q_{max} = 0.29; K_d = 6E6; APSM-18N T_1 Q_{max} = 0.27; K_d = 2E6. (C) CM T_2: Q_{max} = 0.34; K_d = 3E5; APCM-12N T_2: Q_{max} = 0.35; K_d = 5E5; APCM-18N T_2: Q_{max} = 0.31; K_d = 3E5. (D) SM T_2: Q_{max} = 0.26; K_d = 1E6; APSM-12N T_2: Q_{max} = 0.24; K_d = 9E5; APSM-18N T_2: Q_{max} = 0.31; K_d = 2E5.

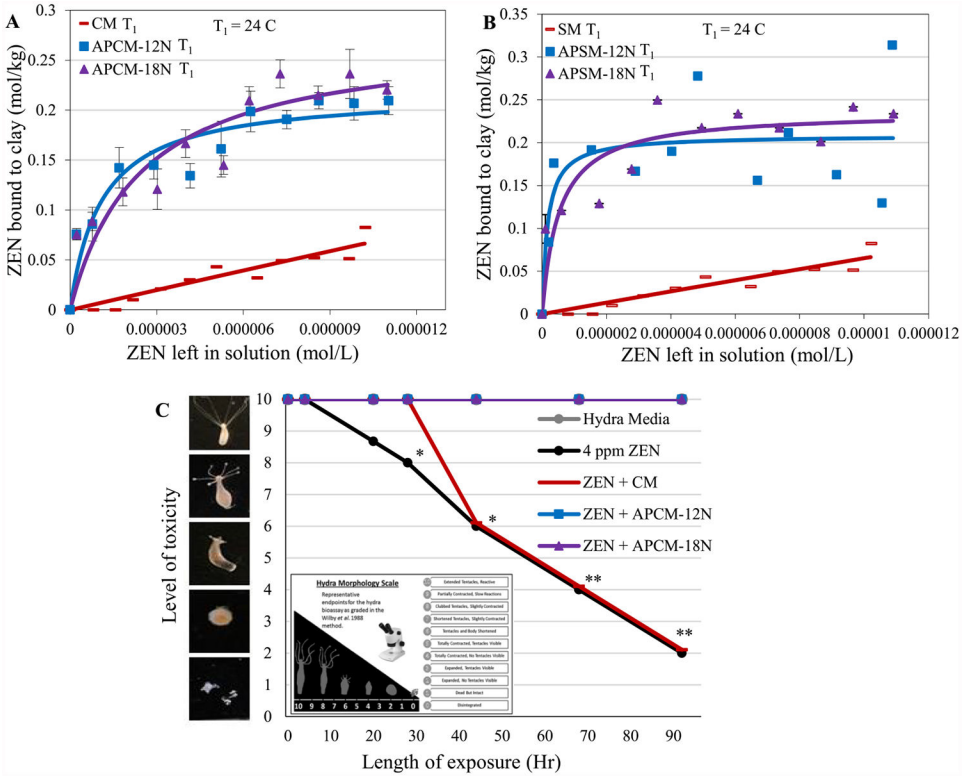

Figure 4.

Langmuir plots of ZEN on APCM (A) and APSM (B) versus parent clays showing the predicted Q_{max} values at 24 °C (T_1). Hydra toxicity and protection by CM and APCM at 0.01% inclusion level against 4 ppm ZEN (C). Hydra media and toxin controls are included for comparison. The score of 10 (indicating no toxicity) contains the hydra media and both APCM treatments (*$P \leq 0.05$, **$P \leq 0.01$). The binding and affinity parameters are as follows: (A) APCM-12N T_1: Q_{max} = 0.22; K_d = 1E6; APCM-18N T_1,: Q_{max} = 0.28; K_d = 4E5. (B) APSM-12N T_1. Q_{max} = 0.21; K_d = 6E6; APSM-18N T_1. Q_{max} = 0.24; K_d = 2E6.

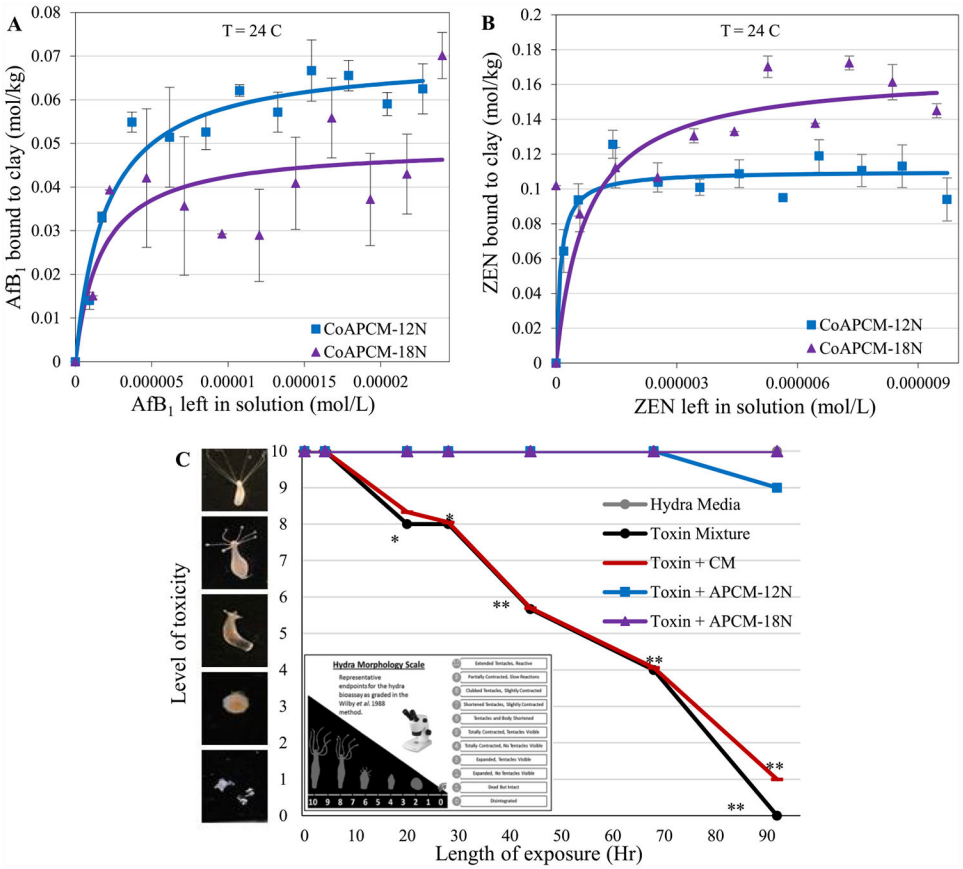

Figure 5.

Langmuir plots of AfB_1 (A) and ZEN (B) on collapsed (Co) APCM. The Q_{max} values indicated tight binding. Hydra toxicity and protection by CM and APCM at 0.1% inclusion level against the toxin mixture (6 ppm ZEN and 1 ppm AfB_1,) (C). Hydra media and toxin controls are included for comparison. The score of 10 (indicating no toxicity) contains the hydra media and APCM-18N treatment (*$P \leq 0.05$, **$P \leq 0.01$). The binding and affinity parameters are as follows: (A) CoAPCM-12N: Q_{max} = 0.07**; K_d = 5E5; CoAPCM-18N: Q_{max} = 0.05**; K_d = 6E5. (B) CoAPCM-12N: Q_{max} = 0.11*; K_d = 9E6; CoAPCM-18N: Q_{max} = 0.17*; K_d =1E7.

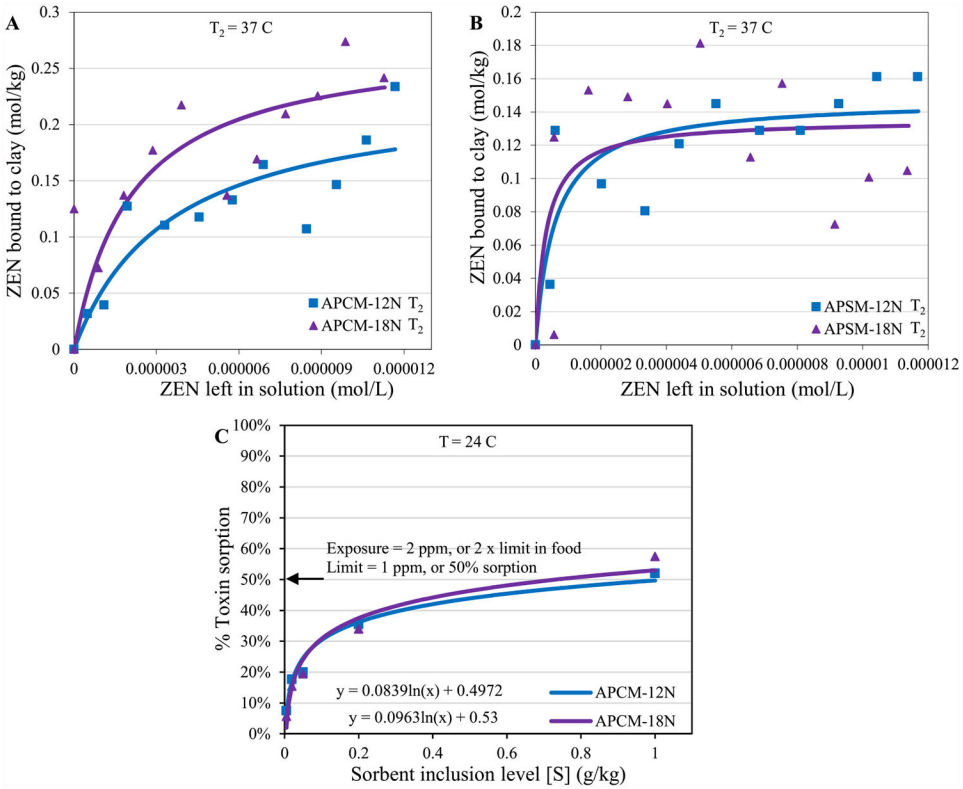

Figure 6.

Langmuir plots of ZEN on APCM (A) and APSM (B) showing the predicted Q_{max} values at 37 °C (T_2). Extrapolation of sorbent dosimetry for ZEN exposure (C). The binding and affinity parameters are as follows: (A) APCM-12N T_2: Q_{max} = 0.23; K_d = 4E5; APCM-18N T_2: Q_{max} = 0.28; K_d = 5E5. (B) APSM-12N T_2: Q_{max} = 0.15; K_d = 2E6; APSM-18N T_2: Q_{max} = 0.14; K_d = 3E6.

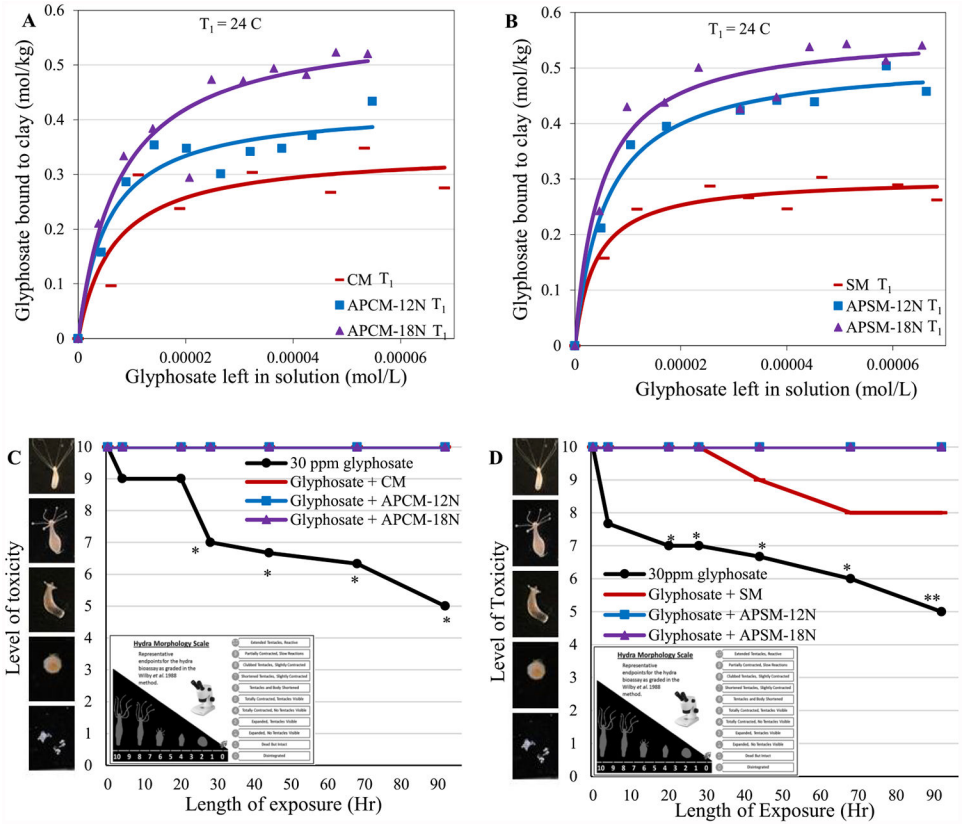

Figure 7.

Langmuir plots of glyphosate on APCM (A) and APSM (B) versus parent clays show the predicted Q_{max} values at 24 °C (T_1). Hydra toxicity and protection by CM and APCM (C), and SM and APSM (D) at a 0.1% inclusion rate are shown against 30 ppm glyphosate. Hydra media and toxin controls are included for comparison. The score of 10 (indicating no toxicity) contains the hydra media and all clay treatment groups except SM (*$P \leq 0.05$, **$P \leq 0.01$). The binding and affinity parameters are as follows: (A) CM T_1: Q_{max} = 0.34; K_d = 2E5; APCM-12N T_1: Q_{max} = 0.42; K_d = 2E5; NSP-18N T_1: Q_{max} = 0.58; K_d = 1E5. (B) SM T_1: Q_{max} = 0.3; K_d = 3E5; APCM-12N T_1. Q_{max} = 0.52; K_d = 2E5; NSP-18N T_1. Q_{max} = 0.56; K_d = 2E5.

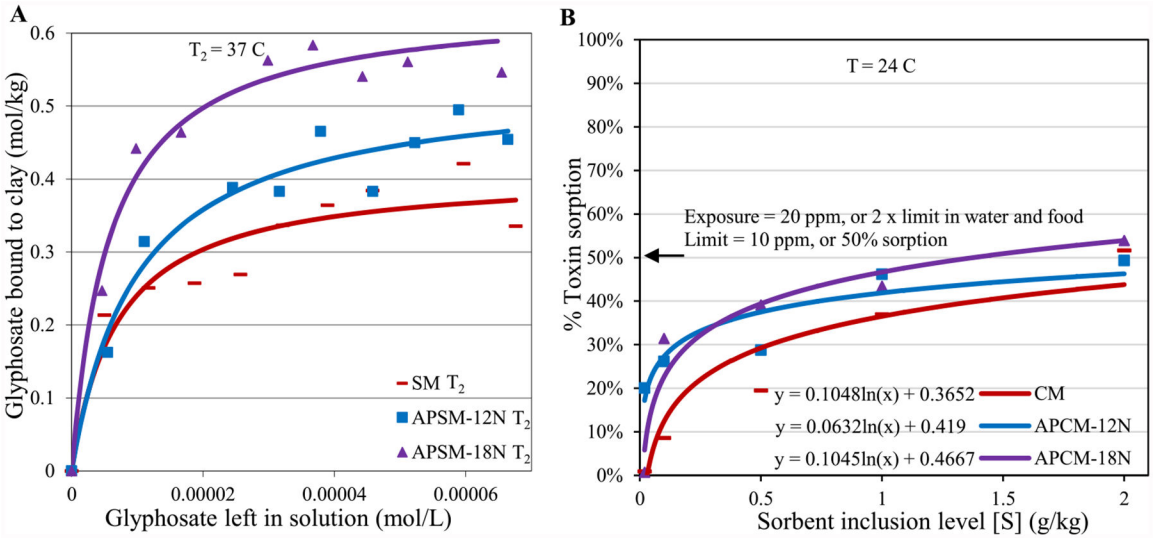

Figure 8.

Langmuir plots of glyphosate on APSM showing the predicted Q_{max} values at 37 °C (T_2) (A). Extrapolation of sorbent dosimetry for glyphosate exposure (B). The binding and affinity parameters are as follows: (A) SM T_2: Q_{max} = 0.26; K_d = 2E5; APSM-12N T_2: Q_{max} = 0.53; K_d = 1E5; APSM-18N T_2: Q_{max} = 0.6; K_d = 2E5.